

Exploiting Latency in Frequency Dependent Networks Equivalents

A. C. S. Lima, F. Camara, F. A. Moreira

Abstract— In this paper we use latency to improve the numerical efficiency of time-domain implementation of pole-residue representation of the nodal admittance matrix in the case of frequency dependent network equivalents. The idea of latency is to use different time-steps for distinct poles, i.e., fast poles are solved using a small time-step while slower poles may be solved using larger time-steps. For the separation of the slow and fast dynamics, a technique named Multiple Companion Networks (MCN) has been developed. The technique has been applied to an open circuit test of a transmission line modeled with a rational model. The results obtained indicated that a gain in numerical efficiency is possible without compromising accuracy.

Keywords: Latency exploitation, frequency dependent network equivalent, transmission line, vector fitting, multiple companion network.

I. INTRODUCTION

RATIONAL modeling is a powerful tool for the realization of frequency dependent networks in electromagnetic transients (EMT) programs such as ATP, EMTP-RV or PSCAD/EMTDC. This procedure allows an efficient implementation of the frequency response in time-domain using recursive convolutions [1] or trapezoidal integration [2]. For the synthesis of the electric network one may use linear or nonlinear techniques. The main drawback of nonlinear techniques is the dependence on the starting point (initial guesses for the poles). For linear techniques, the challenge lies with high order fitting over wide frequency bands.

One procedure that is becoming increasingly more popular is the pole-relocating algorithm known as Vector Fitting (VF) [3]. It is essentially a robust reformulation of the Sanathanan Koerner iteration [4] that uses rational basis functions (partial fractions) instead of polynomials, and pole relocation instead of weighting. The VF algorithm has been applied to transmission lines [5], wide-band transformer modeling [6] as well as frequency dependent network equivalent (FDNE) [7]. The approach allows for high order functions using only stable poles and a wide frequency band. Recently, improvements and extensions have been proposed for VF [8][9]. Even though only stable poles are used, the overall model may not be passive and a post-processing

routine is needed to enforce passivity [10][11][12][18].

In the case of frequency dependent network equivalents (FDNE) the admittance matrix, \mathbf{Y} , is subjected to a rational modeling. This procedure allows to a direct integration to EMTP-type programs as the FDNE can be seen as a black-box connected to an external network. The rational fitting of FDNE is often characterized by a large ratio between the largest and smallest eigenvalues. The high frequency oscillations may demand a small time-step forcing a wideband modeling of the network and leading to a high order transfer function in either the S-domain (Laplace transform) or the discrete Z-transform. Typically a FDNE can be characterized as a stiff system with poles that may differ by several orders of magnitude. The time-step must be small enough to give a good resolution of the high frequency components in the FDNE. By a suitable usage of the concept of latency [13], i.e., multirate simulation, it is possible to improve this situation leading to a more efficient use of computational resources. The use of latency to achieve a higher computational performance has been focused mainly in VLSI circuit using waveform relaxation [14] and in some applications in power systems using the concept of Multi-area Thevenin Equivalents (MATE) [15]. In waveform relaxation each subsystem uses the previous iterate waveforms as “guesses” for the current state of the other subsystems. After that, iterations are performed to match the solutions at all interfacing points. This intrinsic iterative nature of the technique imposes limitations, particularly in the context of real-time simulation and multi-computer simulation environments. In MATE, circuit latency has been exploited using a direct simultaneous solution for the branch currents linking the subsystems. Accurate and efficient results have been reported for the simulation of networks containing transmission lines that decouple fast and slow areas and also for HVDC power converters where the correct representation of the dynamics of the switching valves requires very small time-steps while the remaining of the network may be simulated with larger time-steps. After each subnetwork has been separately solved with its own technique, a Thevenin equivalent of that subnetwork is obtained. The Thevenins of all subnetworks are then brought together and solved for the currents in the link branches. Finally, these link currents are injected back into the individual subnetworks to take into account the fact that they are not isolated.

In this paper we propose a distinct scheme. Instead of using MATE we use the concept that we defined as Multiple Companion Networks (MCN). As it is based on companion networks, i.e., Norton equivalents, it does not require a series link to connect the “fast” part of the network with the one with

This work was supported by INERGE, CNPq – Conselho Nacional de Pesquisa e Desenvolvimento, Brasília, Brazil and CAPES (Coordenação de Apoio a Formação de Pessoal d Nível Superior, Brasília, Brasil). A. C. S. Lima and F. Camara are with Federal University of Rio de Janeiro, RJ, Brazil (e-mail: acsl@dee.ufrj.br, fcamara@ufrj.br). F. Moreira is with Universidade Federal da Bahia, Salvador, BA, Brazil (e-mail: moreira@ufba.br).

“slow” dynamics. It can deal with a network without a “tearing” it in parts. To illustrate the methodology we apply MCN to the rational modeling of the admittance matrix of an untransposed overhead line.

II. RATIONAL FITTING OF OVERHEAD LINE ADMITTANCE MATRIX

The nodal admittance of a transmission line has the structure shown in (1)

$$\mathbf{Y}_n = \begin{bmatrix} \mathbf{Y}_{SS} & \mathbf{Y}_{SR} \\ \mathbf{Y}_{RS} & \mathbf{Y}_{RR} \end{bmatrix} \quad (1)$$

The system in (1) is symmetric and passive so $\mathbf{Y}_{SR} = \mathbf{Y}_{RS}^T$ and has the same structure of a FDNE. In the case of a uniform line there are only two “types” of block matrices, i.e., $\mathbf{Y}_{SS} = \mathbf{Y}_{RR}$ and $\mathbf{Y}_{SR} = \mathbf{Y}_{RS}$ and the following applies

$$\mathbf{Y}_n = \begin{bmatrix} \mathbf{Y}_s & \mathbf{Y}_m \\ \mathbf{Y}_m & \mathbf{Y}_s \end{bmatrix} \quad (2)$$

The block matrices in (2) are defined as

$$\begin{aligned} \mathbf{Y}_s &= \mathbf{Y}_c (\mathbf{I} + \mathbf{H}^2) (\mathbf{I} - \mathbf{H}^2)^{-1} \\ \mathbf{Y}_m &= -2\mathbf{Y}_c (\mathbf{I} - \mathbf{H}^2)^{-1} \end{aligned} \quad (3)$$

where \mathbf{Y}_c is the characteristic admittance matrix and \mathbf{H} is the propagation matrix also known as voltage deformation matrix. The characteristic admittance and the propagation matrices can be obtained using modal decomposition or Schür decomposition. The usage of Schür decomposition allows for a phase-domain approach without resorting to modal decomposition [16].

As is the case of nodal admittance matrix using the Folded Line Equivalent [17], we have to force the approximated functions to be asymptotically correct. Thus the functions to be fitted are in the form

$$\mathbf{Y}_{n_{eq}} \equiv \sum_{n=1}^N \frac{\mathbf{R}_n}{j\omega - a_n} + \bar{\mathbf{Y}}_{CC}(\infty) \quad (4)$$

where $\bar{\mathbf{Y}}_{CC}(\infty)$ is a real block diagonal matrix related to the characteristic admittance at infinite frequency. For the evaluation of the characteristic admittance matrix we have considered 100 MHz instead of infinite frequency.

$$\bar{\mathbf{Y}}_{CC}(\infty) = \begin{bmatrix} \Re(\mathbf{Y}_c(\infty)) & 0 \\ 0 & \Re(\mathbf{Y}_c(\infty)) \end{bmatrix} \quad (0)$$

The rational model was applied to $\mathbf{Y}_{n_{eq}} - \bar{\mathbf{Y}}_{CC}(\infty)$ using a zero constant term and the inverse of the magnitude of each element as weighting. The model was obtained using the *Matrix Fitting Toolbox* (available at the Vector Fitting website:

<http://www.energy.sintef.no/Produkt/VECTFIT/index.asp>).

This procedure was applied in the fitting of an untransposed 10 km, 230 kV line using a combination of linearly and logarithmically spaced samples between 1 Hz and 50 kHz. A total of three thousand samples were used. This large number of samples is needed to resolve the frequency domain

functions. An accurate fitting was obtained using 54 poles with 20 poles being real. The pole map is depicted in Fig.1. The passivity enforcement was only possible using a 64bits MATLAB. The 32 bits passivity enforcement fails due to memory limits. The conductor data of the transmission line as well as the data for the ground are shown in appendix A.

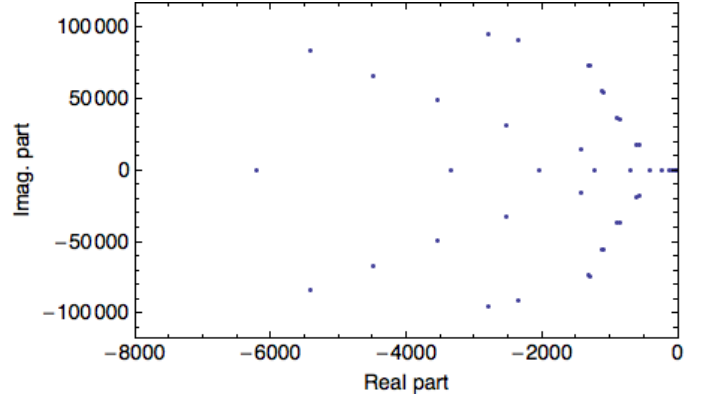


Fig. 1. Pole map for the considered FDNE

III. MULTIPLE COMPANION NETWORKS

The idea behind MCN can be understood as a dual implementation of MATE without demanding a link to interconnect the fast and slow parts of the network. In MATE the structure is essentially the one shown in Fig. 2. A series element is needed to connect both networks and interpolation of the historic voltage source may be needed.

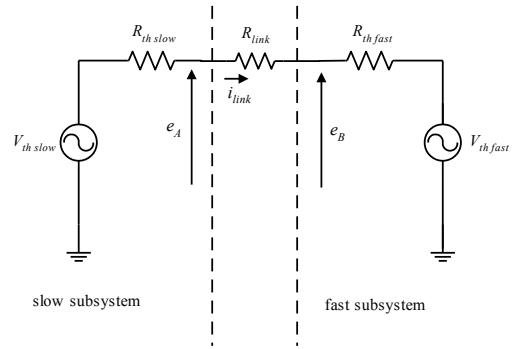


Fig. 2. Basic structure of the MATE algorithm where the equivalents are connected by a series element.

In MCN we take advantage of the companion network realization of convolution-based models. In MCN, the rational model of (4) is divided in two parts each being implemented as an independent Norton equivalent, hence the name MCN. Using recursive convolution or trapezoidal integration allows the model in (6) to be connected to any EMTP-type program equivalent [1][2][7] leading to the equivalent circuit in Fig. 3.

$$\mathbf{Y}_{n_{eq}} \equiv \sum_{n=1}^{N_{fast}} \frac{\mathbf{R}_{n_{fast}}}{j\omega - a_{n_{fast}}} + \sum_{n=1}^{N_{slow}} \frac{\mathbf{R}_{n_{slow}}}{j\omega - a_{n_{slow}}} + \bar{\mathbf{Y}}_{CC}(\infty) \quad (5)$$

In the discretization process both fast and slow subnetworks will create an equivalent conductance that can be directly inserted in the system nodal admittance matrix before entering

the time-step loop. See Appendix B for details in the discretization process. The current source associated with the slow poles is only updated every k -time-step while the one associated with the fast mode is updated every time-step, with k being a natural number, as depicted in Fig.4.

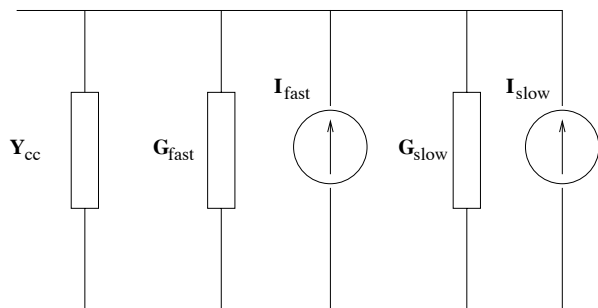


Fig. 3. MCN circuit

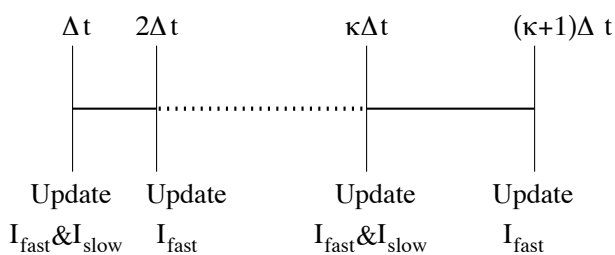


Fig. 4. Timeline for updating the current sources in MCN

IV. TIME-DOMAIN RESPONSE

For the time-domain we consider the case of an open circuit test. A step voltage is applied at one of the phases of the sending end while the other phases are grounded via a small resistance. All phases of the receiving end are open. The transmission line is modeled as a rational model as shown in Fig. 5.

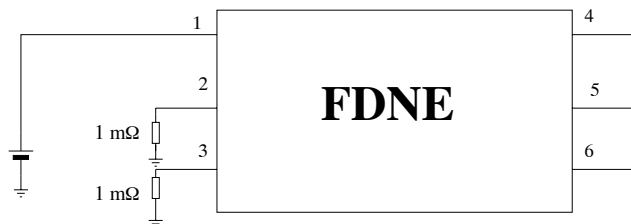


Fig. 5. Time-domain circuit for the evaluation of the latency in a FDNE

In Fig. 6 we show the voltages at terminals 1, 4, 5 and 6, when the FDNE is modeled as a single companion network. Due to the finite frequency band of the FDNE, the time domain responses are prone to Gibbs oscillation. To avoid these oscillations one may resort to a filter as shown in [19].

The whole system was implemented in MATHEMATICA using an approach similar to the Mat-EMTP [20]. A time-step of $1 \mu s$ was used. The total simulation time was 13.968077 s using a 2x2.26 GHz quad-core Intel Xeon processor with 6GB of RAM.

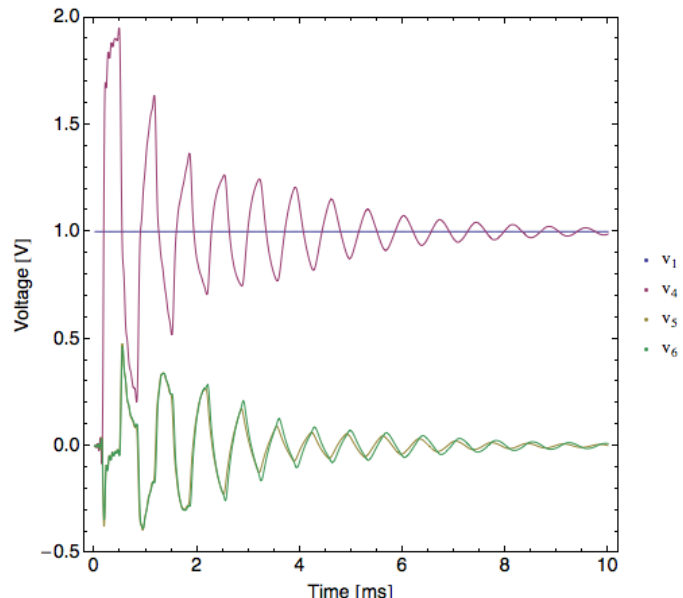


Fig. 6. Time-domain response for a step voltage test

One key point in latency exploitation is the definition of the slow and fast parts of the network. A discussion of some of this issue is found in [15]. When rational modeling is considered, the division of the network is essentially straightforward. As real and complex poles are involved, we postulate that the slow part of the network may only deal with real poles. The tests we carried out indicate that the real poles presented a smaller time constant, thus they can be realized with a higher time-step.

We assume that fast poles present high frequency components thus requiring complex conjugate poles. As previously mentioned the FDNE has 20 real poles and 17 pairs of complex conjugate poles. Thus for a first approximation we start using

$$N_{fast} \leq N - N_{slow}$$

where $N_{slow} \leq 20$ is the number of slow poles and N is the total number of poles.

We used MCN to investigate the maximum number of poles associated with the slow subnetwork as well as the maximum ratio, k , between the slow and fast time-steps. In Fig. 7, it is depicted the absolute value of the largest mismatch found as a function of the number of poles in the slow part of the network (SP) when $k=5$. The voltage with the larger ratio is the one in terminal 4. Fig. 8 shows the same results when the network has a larger number of slow poles. The use of 40 slow poles is just to show that there are some complex poles that contribute to the slow part of the network.

From these two figures it is possible to note that the error is basically monotonically increasing whenever only real poles are considered. If complex poles are considered in the slow part of the network a decrease in the mismatch is found. This result seems to indicate that it is possible to mix real and complex poles in the slow part of the network. Probably a distinct division of the network using only a few real poles and

the low frequency complex poles might give an accurate response as well. This topic in particular is left for future research.

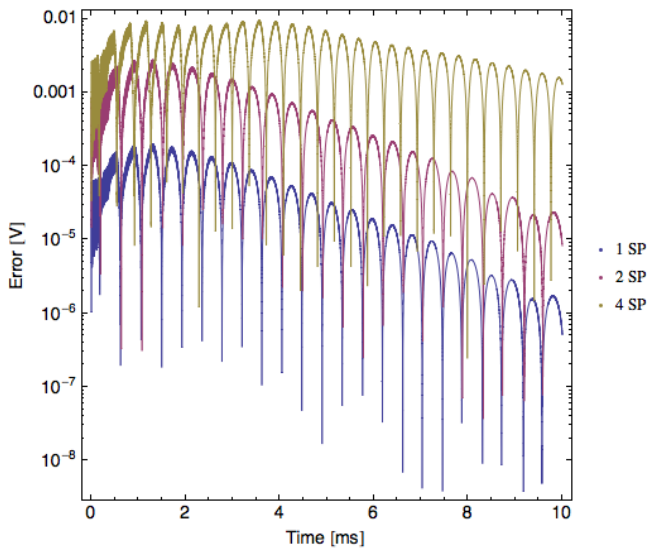


Fig. 7. Absolute value of relative error (mismatch) for time-domain responses using different number of slow poles using $k=5$.

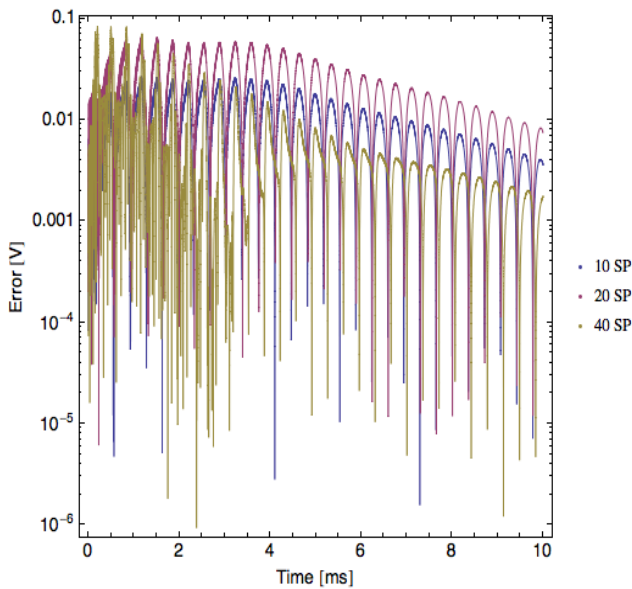


Fig. 8. Absolute value of relative error (mismatch) for time-domain responses for larger number of slow poles using $k=5$.

Fig. 9 depicts the maximum mismatch found considering up to 10 real poles as part of the slow subnetwork and $k=10$. It can be seen that the mismatch is not heavily affected by this change in k . However as k increases there is a significant change in the maximum error found. Fig. 10 summarizes these findings where it can be seen that as the number of poles in the slow part of the network increases, if ratio k also increases, there is a considerable rise in the maximum value of the error.

Table I summarizes the numerical performance of the MCN considering different number of slow poles and $k=5$ and $k=10$. Despite the increase in the error, with a higher number of poles in the slow part of the network there is also an increment in the numerical performance of the MCN.

TABLE I – COMPUTATIONAL PERFORMANCE OF THE MCN REALIZATION OF THE FDNE

# of slow poles	$k=5$	$k=10$
1	13.941769	13.796345
2	13.859429	13.510032
4	13.298749	13.152875
10	12.190794	11.803534
12	11.815353	11.455727
14	11.336278	10.957989
16	11.034261	10.452221
18	10.492678	10.154645
20	10.259190	9.584601

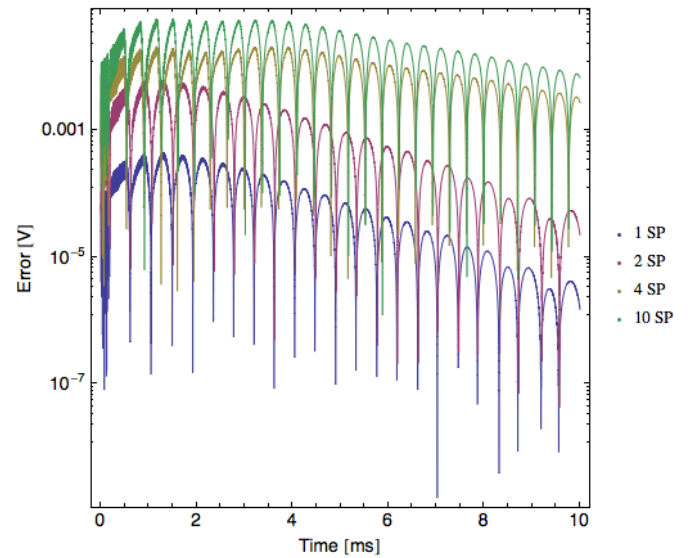


Fig. 9. Absolute value of relative error (mismatch) for time-domain responses using different number of slow poles using $k=10$.

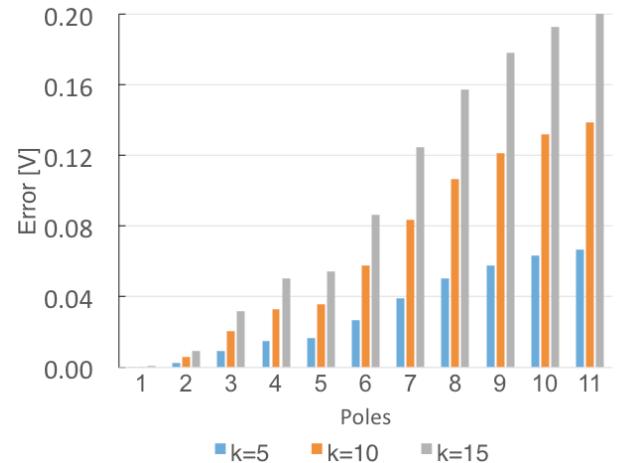


Fig. 10. Maximum error found as a function of the number of poles in the slow part of the network and the ratio k .

V. CONCLUSIONS

In this paper we have dealt with the application of latency in a rational modeling of a frequency dependent network equivalent (FDNE). It uses a concept called Multiple

Companion Networks. It shows that unlike conventional latency applications, the “tearing” of the network in slow and fast parts is very simple. The MCN does not require interpolation in distinct parts of the network.

The procedure was applied in the rational modeling of the nodal admittance matrix of an overhead line. There is a clear tradeoff between accuracy and the number of poles in the slow part of the network and the ratio between the time-steps of the slow and fast parts of the network. For an accurate modeling of the network the computational gain was around 15%. We believe that parallel algorithms, usage of a computer language or FPGA and further investigation of the “tearing” of the network may improve this result.

Further development is needed to assess how the MCN will perform in more complex networks. There is also a need to develop a procedure to optimally define the tearing of the network.

VI. APPENDIX A – CONDUCTOR AND GROUND DATA

The phase conductors have a radius of 2.54 cm and the ground wires are 3/8” EHS. The conductors x and y coordinates are shown below and the ground resistivity is 1000 ohms.meter.

$$\mathbf{x}_c = \begin{bmatrix} -10 & 0 & 10 & -7 & 7 \end{bmatrix}$$

$$\mathbf{y}_c = \begin{bmatrix} 15 & 15 & 15 & 22 & 22 \end{bmatrix}$$

VII. APPENDIX B – CONVOLUTION BASED MODELS

Rational models can be implemented in an ETMP-type program via direct integration of the state equation. For instance, consider a first order system with a real pole, a , real residue, r , and a direct term, d , as shown below

$$y = \left(\frac{r}{s+a} + d \right) u \quad (\text{B.1})$$

with input u (voltage) and output y (current). In the time domain (B.1) can be written as

$$\dot{x} = ax + u \quad (\text{B.2})$$

$$y = rx + du$$

Either applying the trapezoidal integration rule or recursive convolution leads after some manipulation to (B.3).

$$x(n) = \alpha x(n-1) + u(n-1) \quad (\text{B.3})$$

$$y(n) = c x(n) + g u(n)$$

Using recursive convolution the following coefficients are obtained

$$\alpha = \exp(a \Delta t) \quad \lambda = -\frac{1}{a} \left(1 + \frac{1-\alpha}{a \Delta t} \right) \quad \mu = \frac{1}{a} \left(\alpha + \frac{1-\alpha}{a \Delta t} \right) \quad (\text{B.4})$$

$$g = r \lambda + d \quad c = r (\alpha \lambda + \mu)$$

in case the trapezoidal rule is used we have

$$\alpha = \frac{1+a \Delta t / 2}{1-a \Delta t / 2} \quad \lambda = \mu = \left(\frac{\Delta t / 2}{1-a \Delta t / 2} \right) \quad (\text{B.5})$$

REFERENCES

- [1] A. Semlyen, A. Dabuleanu, “Fast and accurate switching transient calculations on transmission lines with ground return using recursive convolutions,” *IEEE Trans. Power App. And Systems*, vol. 94, pp. 561–571, Apr. 1975.
- [2] T. Noda, “Identification of a multiphase network equivalent for electromagnetic transient calculations using partitioned frequency response,” *IEEE Trans. Power Delivery*, vol. 20, no. 2, pp. 1134–1142, Apr. 2005.
- [3] B. Gustavsen and A. Semlyen, “Rational approximation of frequency domain responses by vector fitting,” *IEEE Trans. Power Delivery*, vol. 14, no. 3, pp. 1052–1061, Jul. 1999.
- [4] B. Gustavsen, “Improving the pole relocation properties of vector fitting,” *IEEE Trans. Power Delivery*, vol. 21, no. 3, pp. 1587–1592, Jul. 2006.
- [5] A. Morched, B. Gustavsen and M. Tartibi, “A universal model for accurate calculation of electromagnetic transients on overhead lines and underground cables,” *IEEE Trans. Power Delivery*, vol. 14, no. 3, pp. 1032–1038, Jul. 1999.
- [6] B. Gustavsen, “Wide band modeling of power transformers,” *IEEE Trans. Power Delivery*, vol. 19, no. 1, pp. 414–422, Jan. 2004.
- [7] B. Gustavsen, “Rational approximation of frequency dependent admittance matrices,” *IEEE Trans. Power Delivery*, vol. 17, no. 4, pp. 1093–1098, 2002.
- [8] D. Deschrijver, B. Gustavsen, T. Dhaene, “Advancements in iterative methods for rational approximation in the frequency domain,” *IEEE Trans. Power Delivery*, vol. 30, no. 2, pp. 216–225, May 2007.
- [9] B. Gustavsen and A. Semlyen, “Enforcing passivity for admittance matrices approximated by rational functions,” *IEEE Trans. Power Systems*, vol. 16, no. 1, Feb. 2001.
- [10] A. Semlyen and B. Gustavsen, “A half-size singularity test matrix for fast and reliable passivity assessment of rational models,” *IEEE Trans. Power Delivery*, vol. 24, no. 1, pp. 345–351, Jan. 2009.
- [11] B. Gustavsen, “Fast passivity enforcement for pole-residue models by perturbation of residue matrix eigenvalues,” *IEEE Trans. Power Delivery*, vol. 23, no. 3, pp. 2278–2285, Oct. 2008.
- [12] B. Gustavsen and A. Semlyen, “Fast and reliable passivity assessment of rational models,” *IEEE Trans. Power Delivery*, vol. 24, no. 1, pp. 345–351, Jan. 2009.
- [13] R. A. Saleh, A. R. Newton, “The exploitation of latency and multirate behavior using nonlinear relaxation for circuit simulation,” *IEEE Trans. Computer-Aided Design*, vol. 8, no. 12, pp. 1286–1298, Dec. 1989.
- [14] E. Lelarasmee, A. E. Ruehli, A. L. Sangiovanni-Vincentelli, “The waveform relaxation method for time-domain analysis of large integrated circuits,” *IEEE Trans. Computer-Aided Design*, vol. 1, pp. 131–145, July 1982.
- [15] F. Moreira, J. Marti, L. Zanetta Jr., L. Linares, “Multirate simulations with simultaneous solution using direct integration method in a partitioned network environment,” *IEEE Trans. on Circuits and Systems*, vol. 53, no. 12, pp. 2765–2778, Dec. 2006.
- [16] A. Lima, C. Portela, “Inclusion of Frequency-Dependent Soil Parameters in Transmission-Line Modeling,” *IEEE Trans. on Power Delivery*, v. 22, n. 1, pp. 492–499, Jan. 2007.
- [17] B. Gustavsen, A. Semlyen, “Admittance-based modeling of transmission lines by Folded Line equivalent,” *IEEE Trans. on Power Delivery*, v. 24, n. 1, pp. 231–239, Jan. 2009.
- [18] B. Gustavsen and A. Semlyen, “Fast and reliable passivity assessment of rational models,” *IEEE Trans. Power Delivery*, vol. 24, no. 1, pp. 345–351, Jan. 2009.
- [19] A. Ubolli, B. Gustavsen, “Multiport frequency-dependent network equivalencing based on simulated time-domain responses,” *IEEE Trans. Power Delivery*, vol. 27, no. 2, pp. 648–657, Apr. 2012.
- [20] J. Mahseredjian, F. Alvarado, “Creating an electromagnetic transients programs in MATLAB: MatEMTP,” *IEEE Trans. Power Delivery*, vol. 12, no. 1, pp. 380–388, Jan. 1997.